Applied Surface Science 307 (2014) 503–512

Contents lists available at ScienceDirect

Applied Surface Science

journal homepage: www.elsevier.com/locate/apsusc

Evaluation of bone tissue reaction in laser beamed implants

Sergio Allegrini Junior[a,*], Marcelo Yoshimoto[a], Marcos Barbosa Salles[b], Marcia Rivellino Facci Allegrini[c], Luciana Crepaldi Yazawa Pistarini[d], Francisco Jose Correa Braga[d], Ana Helena de Almeida Bressiani[d]

[a] Graduate Program in Biodentistry, Ibirapuera University (UNIB), São Paulo, SP, 04661 100, Brazil
[b] Department of Oral and Maxillofacial Surgery, Nove de Julho University (UNINOVE), São Paulo, SP, 02117 010, Brazil
[c] São Paulo Fire Department (SPFD) of the Militar Police, Dentistry Section, São Paulo, SP, 01018 001, Brazil
[d] Nuclear and Energy Research Institute – IPEN/USP, São Paulo, SP, 05508 900, Brazil

ARTICLE INFO

Article history:
Received 27 August 2013
Received in revised form 7 April 2014
Accepted 9 April 2014
Available online 18 April 2014

Keywords:
Laser-treated surface
Biocompatibility
Surface roughness
Oxygen

ABSTRACT

The purpose of this study was to evaluate alterations and bone tissue response on laser treated implant surfaces (Nd:YAG – 100 W). Sixty grade II titanium (ASTM F67) mini-implants (1.5 mm × 4.0 mm) were installed in femurs of 30 Wistar rats. The animals were divided into two groups: thirty mini-implants were machined elements (Machined Group) and the other thirty had laser beamed surfaces (Laser Group). The animals were subdivided into three groups, according to bone healing periods of 15, 30 and 60 days. The samples were analyzed under light, scanning electron and confocal 3D microscopy as well as by EDS (energy dispersive spectroscopy) and Student's *t* test was used for statistical analyses. Light microscopy results showed new bone trabeculae formation toward laser-treated implants at 15 days' bone repair as well as thin layers of osteoid matrix, indicating high biocompatibility. Similar features were observed in the Machined Group but only after 30 days. Bone/implant contact was better evidenced on laser-treated surfaces compared to that on simply machined implants. The only group that demonstrated change in level of significance was the laser-treated group at the 15-day-healing period ($p < 0.05$). Higher oxygen concentration possibly provides more efficient response of osteoblasts during new bone tissue deposition. Implant treated surfaces altered by laser beaming, their composition, surface topography and surface energy may be the future scene in implant dentistry.

1. Introduction

Titanium is considered as "the material of choice" in the manufacturing of dental implants. When a titanium implant is installed in the maxillary or mandible bone, bone cells identify the surface favoring the migration of defense cells, as well as healing cells, toward the substratum. As a result, there is an almost direct biological link between the bone and the metal element, which indicates its biocompatibility.

Medical and Dental Schools are increasingly intertwined in the development of new biomaterials to be used in repairing of human bodily parts, either damaged by accidents or for pathological reasons. Both areas of Health Studies are involved in the search for new technologies, in order to achieve improved response concerning osteoconduction. Titanium alloy is considered to be a metal with excellent biocompatibility [1] and studies have shown that cells perceive differences on surface characteristics and respond in different ways [2–5].

Bone response following anchorage is influenced by the characteristics on implant surfaces. The extent of contact between titanium and new bone depends on characteristics such as the composition of the alloy, surface topography, surface roughness and surface energy of the implant. Chemical composition and surface topography of titanium implants play an important role in the rate and extent of osseointegration as well as adhesion of bone cells onto titanium surfaces [1]. Changes in the configuration of surfaces can alter the targeting of proteins to be adsorbed, as well as the adhesion of certain cells onto the surface [6]. In order to obtain cellular responses that are favorable in terms of bone deposition, modified titanium surfaces have been used. These include hydroxyapatite coated surfaces, Titanium Plasma Sprayed (TPS) surfaces, sand blasted surfaces, acid etched surfaces [7], anodized surfaces (to affect morphological changes) [8] and biomimetic coatings. These surface modifications help bone repair and accelerate mineralization of the osteoid matrix [9].

* Corresponding author. Tel.: +55 11 28932427; fax: +55 11 28932427.
E-mail addresses: sergiojr@usp.br, sergioaj@ig.com.br (S. Allegrini Junior).

http://dx.doi.org/10.1016/j.apsusc.2014.04.065
0169-4332/

Published data on this subject have suggested that tissue cells migrate more easily because of adequate surface tension, which helps promote such migration of new cells for bone deposition [10]. In early stages, this factor may play an important role in discriminating and in determining which proteins should be adsorbed onto the surface, as well as in promoting or inhibiting the adhesion of certain cells. Surface energy can have an effect in the later stages of bone formation and calcification, influencing the types of cells that initially attach to the implant surface and will differentiate at the interface between the titanium element and the bone tissue.

Surface treatment of titanium implants using high-powered laser beaming is an alternative method to obtain morphological changes. Changes produced by this method concerning physical and chemical properties of the surfaces can help promote and accelerate biomechanical anchoring of implants. In addition, this method does not introduce impurities nor gaseous components onto the surface and, thus, it maintains the metal composition unaltered [11]. However, thermal discharges from the laser pulses could alter the composition and microstructure of the implant surface [12].

Nowadays, laser equipment is widely used in Health Fields. Neodymium Yttrium Aluminum Garnet Laser (Nd:YAG - λ = 1.064 nm), CO_2 (carbon dioxide laser – λ = 9.300 nm, 9.600 nm, 10.300 nm and 10.600 nm) and diode laser treatments with wavelengths of 810 nm and 980 nm have been used in the clinical practices of both Medicine and Dentistry [13].

Laser treatments are used in photocoagulation of blood vessels in treatments of tumors, ocular surgery, vaporization of tissue and kidney stones, removal of skin blemishes or tattoos, in rejuvenating treatments, permanent hair removal, healing of ulcers and bleeding, as well as in the removal of decayed dental tissues [13].

Several advantages are highlighted by the use of laser devices in the oral cavity such as easier control of hemostatic effects and bactericidal effects against periodontal pathogens. However, several potential risks may indicate against high power laser in clinical uses. It was demonstrated in studies of root surface that Nd:YAG laser penetrates the tissue to a depth that can cause damage to the respective underlying layers [14].

The Nd:YAG laser beaming is not suitable for treatments on metal contaminated surfaces (*e.g.* peri-implantitis) because it causes overheating and possible melting of components [12]. The high-intensity Nd:YAG laser was used in studies to modify surfaces of titanium implants [12] where, due to the rapid temperature rise, it generated alterations on their original morphology. Even procedures in light emission energy present considerable risks. A study [15] described the effects of laser treatment with Nd:YAG *in vitro* on the properties of surface plasma spraying on titanium and also hydroxyapatite-coated implants. Effects on the surfaces were examined after laser treatment with 0.3, 2.0 and 3.0 W. Results showed loss of fusion, porosity and surface alterations on the model surfaces of both treatments, even under low power. In another study focused on oxidation, promoted by the impact of laser beams on titanium surfaces, the authors concluded that the oxide layer thickness was modified and that the metal fused due to the amount of emission in one same place [16].

Laser ablation changes the microstructure and increases hardness. Further, it alters roughness, improves corrosion resistance and increases surface oxide thickness [11]. A network of micro craters is formed [12] because of heat stress from laser irradiation [11]. These changes to the surfaces of endo-osseous implants can affect the biological behavior of bone tissue [8] by changing the direction of osteoblasts movement, thus favoring the control of growth direction [2].

Studies about the physical alterations that metallic components undergo when laser is processed in oxygen environments have been the subject of several investigations [11,12,17]. Laser irradiation of metallic surfaces in oxidizing environments (oxygen or air) causes changes in oxide growth at regions upon which the laser beam is incident. Rapid oxidation of the metal surface is considered to occur due to energy release [17]. According to György et al. [12], laser pulses applied to titanium surfaces increase the surface temperature causing the melting of the surface layer, which subsequently solidifies, promoting increased oxidation. The most important effect observed at the target region is the increased oxide layer thickness [11,17], which is due to the release of heat during the oxidation reaction [12].

Rats are favorable, as animal models, due to their small size, low cost and stable metabolism. The animal model used in this study was considered suitable due to the size of the femoral bone according to the mini-implants used, allowing installation at a regular and standardized distance, in proportion to the walls of the femur bone of the animal. Furthermore, selected rats weighing approximately 350 g, in average 9 to 10 weeks old, are considered "adults" when compared to human beings, allowing similar biological comparison to the metabolism of an adult man.

Based on the biological potential of surfaces that have undergone modifications, brought about by various treatments, during the last 10 years, and with the idea of improving and accelerating bone-implant interaction, the purpose of this study was to evaluate the biological response of bone tissue *in vivo*, when using implant surfaces that have been morphologically altered by laser beaming. This response has been compared to that on simply machined surfaces.

The purpose of this study also aimed to a better understanding of the changes that take place in the surface oxide layer with the aid of scanning electron microscopy (SEM) and energy dispersive spectroscopy (EDS).

2. Materials and methods

In this study, 60 sterile* mini-implants in grade II titanium (ASTM F67), standard size of 1.5 × 4.0 mm Ø, were installed in the femurs of 30 Wistar rats.

*The evaluation of the endotoxin content in the samples after sterilization by gamma radiation from ^{60}Co was conducted *via* VDMAX (Maximum Verification Dose) method to control the microbial load (bioburden) according to ISO 11137. The result was zero colony forming units (CFU) of microorganisms under irradiation at 25 kGy in 10 units (within same batch of implants used in this research), which also confirmed no presence of endotoxin generator vectors.

Initially, the surfaces were analyzed using different techniques (further discussed below) and, subsequently, surgical procedures were carried out in the animals.

The animals were divided into two groups: In Group I (Machined Implants Group), 30 (thirty) implants with machined surfaces were used while, in Group II (Laser-treated Implants Group), the other 30 (thirty) machined implants had their surface subjected to irradiation with Nd:YAG Laser equipment in order to create and increase surface roughness.

Each of the two groups (Group I and Group II) was randomly divided into 03 (three) distinct sub-groups according the respective bone healing periods of 15, 30 and 60 days, until the removal of the implant samples for analyses.

2.1. Laser surface preparation

Nd:YAG laser (ADITEK) (Cravinhos, SP) was selected for this study because it provides a degree of average power, suitable for engraving and marking surfaces, with limited penetration of less than 1 mm and the ablation process

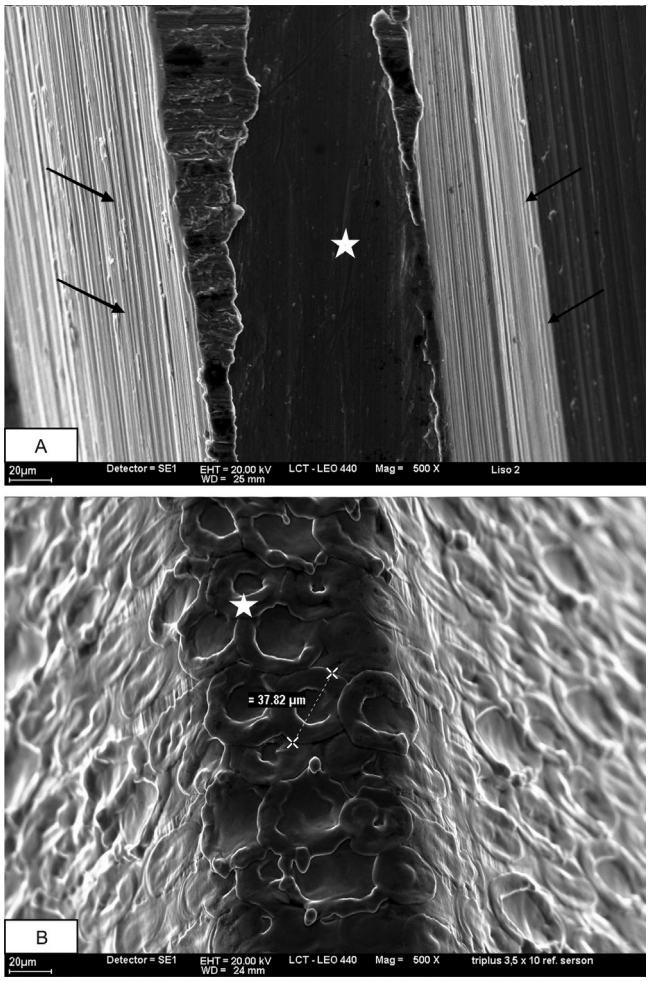

Fig. 1. (A) SEM image of a spiral where grooves caused by machining (arrows) in the region of the flanks can be observed. The white star indicates the crest area of the implant where EDS analysis was conducted (Spectrum I). (B) SEM image of the crest surface area in a laser-treated sample. A crater formed by the laser pulse was measured and its diameter was of 37.82 μm. The white star indicates the region where EDS analysis was conducted (Spectrum II).

without generating topographic edges. This equipment presented the following characteristics: Pulse energy = 0.56 mJ; Pulse width = 10 ns; Peak power = 5.6×10^4 J/s; Average power = 3.8 J/s; Fluency = 0.311 J/mm^2.

The laser-treated implant surfaces were prepared according to the following parameters: Irradiation angle = 5°, Distance between laser beam release and implant surface = 100 mm, Procedure mode = transversal scanning in relation to the axis of the implant, Wavelength = 1064 nm, Pulse frequency = 5 kHz, Scanning speed = 300 mm/s, Space between scanning = 0.01 mm, Interval between pulses = 10 ns (same as pulse width) and Pulse energy = 0.56 mJ.

2.2. Surface analysis

2.2.1. Scanning electron microscopy (SEM) and Energy Dispersive Spectroscopy (EDS)

The titanium implants had machined surfaces (Fig. 1A) and were roughened by laser beaming (100 W Nd:YAG laser) – Fig. 1B. The implant surfaces were analyzed using EDS.[1] The purpose of this analysis was to determine possible changes in the chemical composition generated by the heat released during laser beaming.

Surface morphology was examined by SEM (Stereoscan 440).

2.2.2. Confocal microscope

The morphology of high power laser beamed surfaces was also carefully examined with a 3D confocal microscope (Leica DCM 3D Map[1]).

This type of examination enables the determination of roughness, as well as the length and depth of craters observed on laser treated surfaces.

2.3. Surgical procedures

30 (thirty) Wistar rats, each weighing approximately 350 g were selected. It was stipulated that animals with body weight below 330 g and above 370 g should not be included in order to better control the metabolic response for each animal. Furthermore, it was stipulated as a rule, that, in the left femur, only machined implants were inserted, while, in the right one, only implants undergoing laser treatments were inserted. The animals were derived from the Animal Research Facility of IPEN (Institute of Energy and Nuclear Research). The animals were housed in cages suitably placed in ventilated racks, at a temperature ranging from 20 to 22 °C, with relative humidity between 30 and 70%, in a light–dark cycle of 12 hours daylight, during the entire period of the experiment. All animals used were according to the rules and regulations of FELASA - Federation of European Laboratory Animal Science Associations.

Each animal received two mini-implants. In all the experimental groups, the surgical site was the metaphyseal region of the animal's femur. The initial procedure was the shaving with a sharp blade to expose the skin and the application of an iodine solution. The incision was made in the animal's skin in the proximal-distal direction, and the soft tissue was manipulated for bone exposure. The exposed bone was then perforated by a helicoidal 1.2 mm round drill with abundant saline irrigation, approximately 0.5 cm from the proximal joint. One implant was inserted in each femur. The soft tissues were then closed using standard layered suture techniques. All surgical procedures were performed under anesthesia. Each animal was subject to sedation, analgesia, and muscle relaxation by means of an intramuscular injection (2,2-xylidine) – 5,6-dyhidro-4H-1,3-chlorate thyazyn (Rompum, Bayer, São Paulo, SP, Brazil) (5.0 mg/kg), acepromazine (Acepran® 1% Univet, São Paulo, SP, Brazil) (0.75 mg/kg). For general anesthesia, IM ketamine (Ketamina®, Agener, União Química Farmacêutica Nacional SA, São Paulo, SP, Brazil) (35 mg/kg) was administered. Throughout the whole procedure, the animals were maintained in deep anesthesia for 20–40 min. After post-surgical healing periods of 15, 30 and 60 days, euthanasia was conducted by asphyxiation, through increased concentration of carbon dioxide (CO_2), in proper isolation chambers. This research was conducted with the approval of the Ethical Committee for Animal Research of the Biomedical Sciences Institute/USP (107/03).

2.4. Grinding and polishing

The samples were soaked in methyl methacrylate (Product Number M55909S Sigma Aldrich – St. Louis, MO, USA) – 85 ml, associated with diisobutyl phthalate (Product Number 84-695 Sigma Aldrich) – 15 ml. After the soaking procedure, benzoyl peroxide (1%) was added and the embedded samples were kept at room temperature for a period of 3 days. After that period, the dosage of peroxide was increased to 2.5% and the samples were maintained for two more days. The containers were stored at 37 °C for 3 days or until complete polymerization. The samples were then sectioned (Exakt Apparatebeau, Norderstedt, Germany) along the femur long axis,

[1] Located in the Technology Characterization Laboratory of the Institute of Mines and Petroleum of the Polytechnic School of the University of São Paulo (USP).

according to Donath and Breuner [18]. Due to the diameter of each implant, only two sections were obtained for each sample. The thin sections were attached to acrylic plates with cyanoacrylate cement (Superbonder, Loctite® – Itapevi, São Paulo, Brazil) and then ground and polished (600 to 4000 mesh, grit SiC paper) in a metallographic polishing wheel (Panambra Técnica, São Paulo, Brazil). The non-decalcified final section thickness was of approximately 30 μm. The cutting, grinding and polishing of the samples were all performed under constant water irrigation.

Morphological studies on sections were conducted using light microscopy (Nikon Eclipse E-1000[2] and scanning electron microscopy (Stereoscan 440[1]). Some sections of the laser treated group after 30 days were covered with a layer of carbon, and analyzed using EDS to identify any chemical elements at the bone/implant interface.

2.5. Data analysis

In histomorphometric analysis, counts of the new bone deposited were made only in the space between the two flanks of each central thread on the surface of the implants. Data were collected on both sides of the implant and then analyzed in each photographed section. For this assessment, digital images and computer program Image-Pro Plus (Version 4.1 for Windows) were used. This program allows the quantification of various tissues through the existing pixel color analysis. As a means of statistical analysis, percentage data of new bone deposited obtained by readings for both subgroups – Machined Group (15, 30 and 60 days) and Laser Group (15, 30 and 60 days) – were subjected to Student's *t*-test with significance level ($p < 0.05$). Student's *t*-test is the most frequently adopted statistical method for the evaluation of differences among averages between two groups, even in small quantity samples. For this test, the analyzed data considered the different bone healing periods and the types of implant surfaces.

3. Results

3.1. SEM

SEM examination of the implant surfaces confirmed superficial roughness generated by the machining process and the roughness created during laser beaming.

Fig. 1A shows the usual slots on the flanks of the thread filets generated by the machining process when the implants are manufactured (Machined Implants). In comparison to this, on the laser-treated implant surfaces, craters formed by the laser beaming masked the machining marks (Fig. 1B). The configuration and morphology of the laser treated surface indicates the marked effect of laser pulse energy. Increase in surface temperature during laser treatment results in the melting and evaporation of a thin surface layer of titanium and consequent oxidation. Craters generated by laser beaming can be seen in Fig. 1B and a crater was measured and its diameter was of 37.82 μm.

3.2. Confocal microscope

With the aid of a confocal microscope (Leica DCM 3D Map[1]) images were obtained along with 3D characterization of surface texture and geometry (Fig. 2). This method of evaluation permitted determination of the approximate volume of each crater. This helped determine if the morphology obtained by this method of preparation was adequate in terms of characteristics for accommodation and deposition of bone matrix produced by osteoblasts. For this analysis, three regions distributed across the long axis of the laser implant surface were selected, totalizing 50 craters measured. The average results of this experiment showed contact surface of ~800 μm^2 and total volume of ~2100 μm^3 and maximum depth/height of ~7 μm.

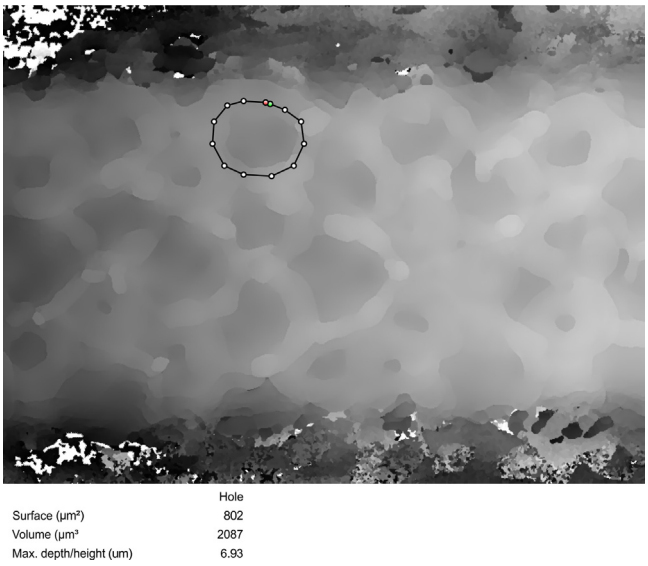

Fig. 2. 3D analysis of the border of a crater that resulted from a laser shot. In the picture, the circumference indicates the representation of a typical laser shot crater measured. The contact surface represented by the volume and maximum depth were determined.

3.3. EDS

For this analysis, 10 measures in three regions in the long axis were assessed, totalizing 30 craters measured for each type of implant. EDS analysis of machined and laser treated surfaces on the crest of the implant spiral (Fig. 3) showed only O and Ti peaks. The oxygen ion concentration on the machined surface was of 4.4 at% and that on the laser beamed surface was of 13.9 at% (Fig. 3).

3.4. Light microscopy

Out of 60 implants used in this study, 120 blades were prepared for histological evaluation. Although, due to the methods of sample preparation, only 109 slides were properly completed, since the remaining ones were damaged/lost during the grinding and polishing of the sections.

At 15-day healing periods, femur samples with machined implants installed were examined in a light microscope (Fig. 4A) and small areas between the inner side of the cortical bone and the body of the implant, filled with yellow bone marrow [*Medulla ossium flava*], were observed, showing scarse bone matrix deposits in this space. Only after 30 days (Fig. 4C), some new bone formation deposits could be seen near the surface, although not fully filled with bone trabeculae.

Evaluation of the laser treated samples revealed contrasting results mainly in the area filled with yellow bone marrow. After repair periods of 15 and 30 days (Fig. 4B and D), accelerated deposition of trabecular bone was evident when compared to the machined implant samples. After 15 days, islands of newly deposited bone tissue could be observed, distributed in a sparse pattern, filling the space between the inner side of the cortical bone and the implant surface (Fig. 4B). After 30 days, the trabeculae

[2] Located in the Laboratory of Neuro Anatomyz. Department of Anatomy Institute of Biomedical Sciences 3 (ICB-3) - USP.

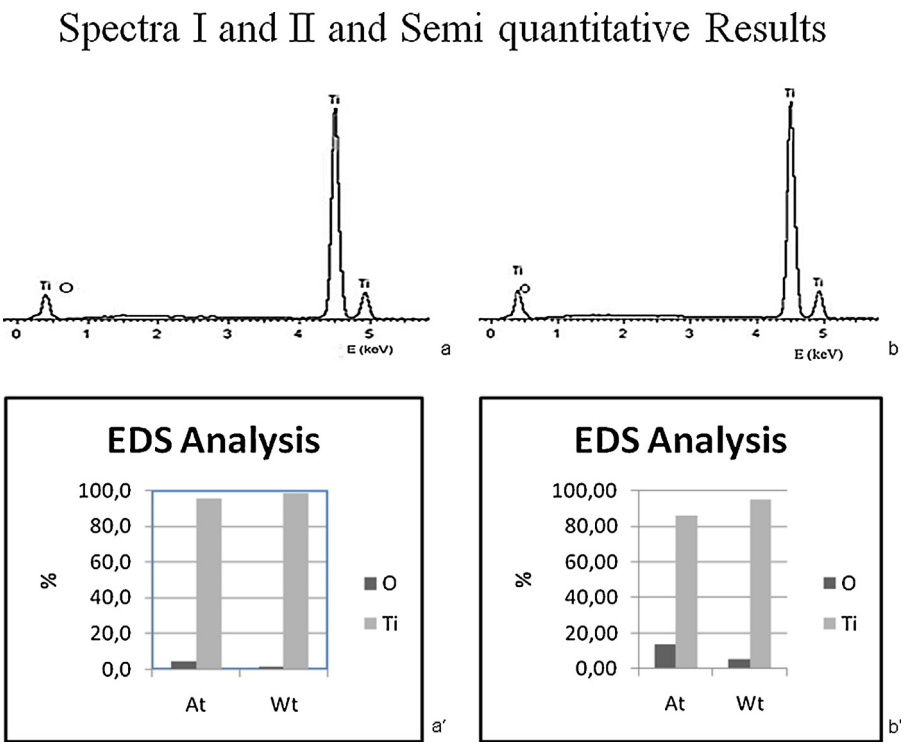

Fig. 3. Spectra I and II. Spectrum I of machined implants (a), spectrum II of laser-treated implants (b) and semi-quantitative energy dispersive X-ray analysis results (a′ and b′) At: Atomic Percent; Wt: Weight Percent; O: oxygen; Ti: Titanium.

became more elongated and interconnected with each other, thus showing remodeling of bone matrix (Fig. 4D).

Comparative analysis of the two types of surfaces showed that in 15 days there was bone/implant contact (Fig. 4B) in the laser treated implants, whereas in the simply machined surfaces this contact was achieved only after 30 days (Fig. 4C).

After 60 days of bone repair, samples from both Groups I and II (Fig. 4E and F) showed no specific differences, which indicated an interval in the process of bone deposition and probably the beginning of the tissue-remodeling phase. Samples of the machined surface implants (Fig. 4E) showed thin layers of new bone tissue interacting with the surface of the titanium substratum. Similar results were observed on the laser-treated implants (Fig. 4F).

Samples of machined and laser-treated implants, after the 30-day healing period, were observed at a higher magnification. The implants responded differently regarding the approximation of trabecular bone.

Group I (Machined Implants) (Fig. 5A) showed no bone/implant contact over the entire surface, while Group II (Laser-treated Implants) (Fig. 5B) indicated increased accommodation of new bone, possibly due to greater roughness on the titanium surface and a larger contact area.

3.5. SEM lamina scanning

Examination of a lamina from Group I at 30-day-repair (Fig. 6A) revealed that the deposited bone tissue was not in contact with the implant surface in the area between two spirals, which can indicate displacement of bone matrix during the grinding process of the laminae. A space of 14.3 μm was measured between the implant and the newly deposited bone tissue. When a lamina of a laser-treated implant from the 30-day-repair group (Fig. 6B) was observed by SEM, it revealed accommodation of newly mineralized bone matrix, due to the higher roughness caused by the high-power laser beaming.

3.6. EDS spectra

The EDS analysis (Fig. 7) shows a carbon peak resulting from the thin carbon layer deposited on the surface of the slides prior to analysis. The spectrum III obtained from the base of a crater caused by a laser pulse shows titanium and significant amounts of oxygen (30.2 at%), calcium (12.9 at%) and phosphorus (6.0 at%), due possibly to the proximity of newly deposited bone. The spectrum IV obtained from a region with newly deposited bone mass revealed 58.3 at% oxygen, 26.8 at% calcium and 14.3 at% phosphorus, which are the main elements of mineralized bone tissue.

3.7. Histomorphometry

Histomorphometric analyses were based on the data concerning newly deposited bone. A total number of 109 sections were analyzed for data acquisition. These data were measured and the averages were obtained from the percentages within the different samples. For Group I (Machined Implants), the percentages showed the following average results in 15 days' time: new bone deposited = 22 with $\sigma = 8$ (Variation Coefficient VC = 38.7%); in 30 days: new bone deposited = 36 with $\sigma = 11$ (VC = 31%); and in 60 days: new bone deposited = 25 with $\sigma = 8$ (VC = 32.9%). And, for Group II (Laser-treated Implants), the results achieved in 15 days were: new bone deposited = 51 with $\sigma = 9$ (VC = 19%); in 30 days: new bone deposited = 44 with $\sigma = 12$ (VC = 28%); and in 60 days were: new bone deposited = 34 with $\sigma = 16$ (VC = 48%). Preliminary evaluations showed better bone deposition on the laser-modified surface at the 15- and 30-day tissue repair phases. In order to verify reliability of the data obtained during the analyses of the samples, a statistical analysis was conducted by Box-plot, where mean values are demonstrated. These results are shown in Fig. 8.

The results obtained later by Student's t test analysis showed significant variations in the amount of newly formed bone between the two groups at 15 days (Machined Group – New Bone

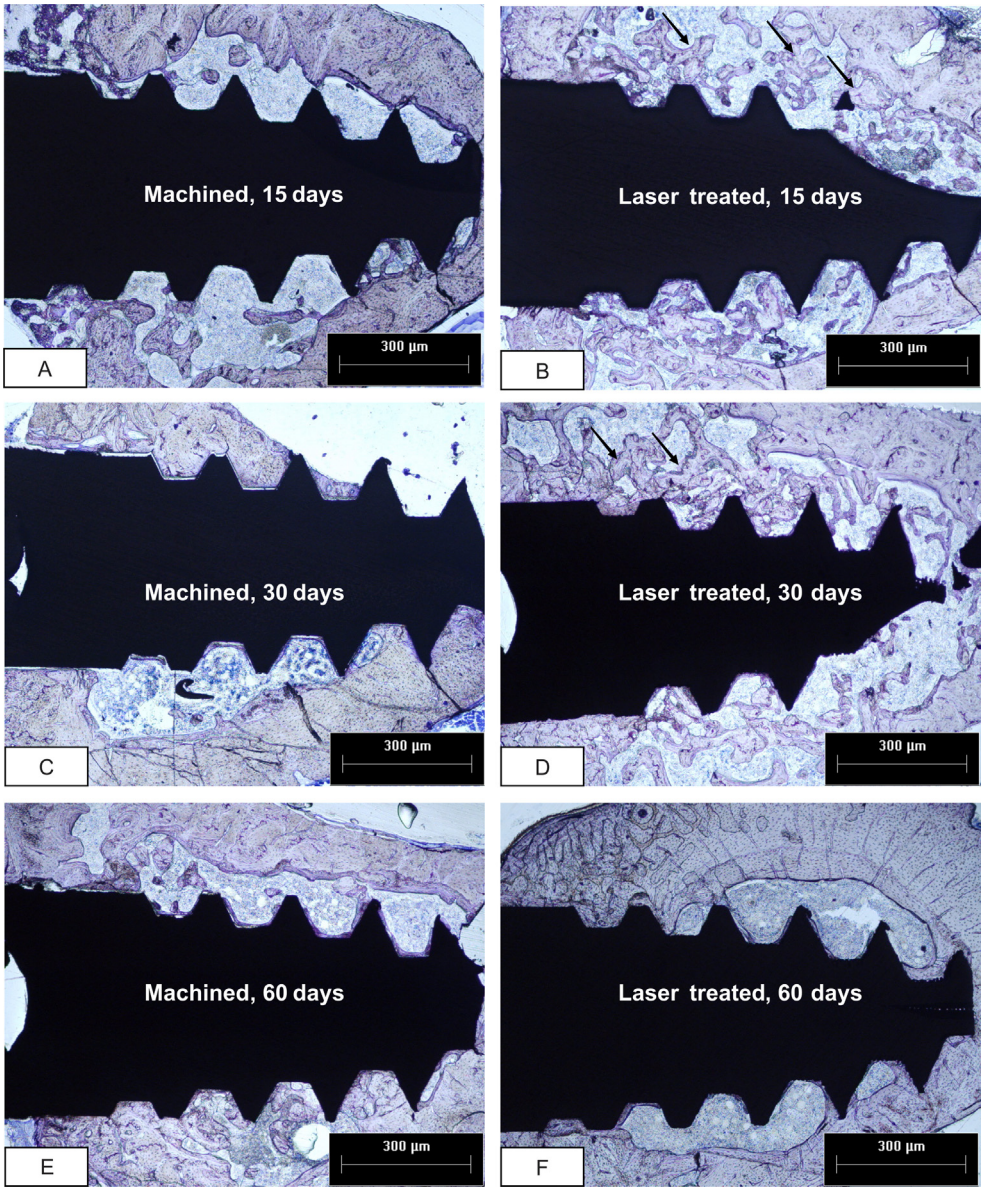

Fig. 4. (A)–(F) Sections under light microscopy. Significant image sections in different animals. During the first 15-day and 30-day healing periods, there was more trabecular bone deposition (arrows) on the laser-treated surfaces (B and D) compared to that observed on the machined surface implants (A and C). When the two types of surfaces were examined after 60 days, no significant differences were observed as for the amounts of bone tissue deposition (E and F). Toluidine blue staining.

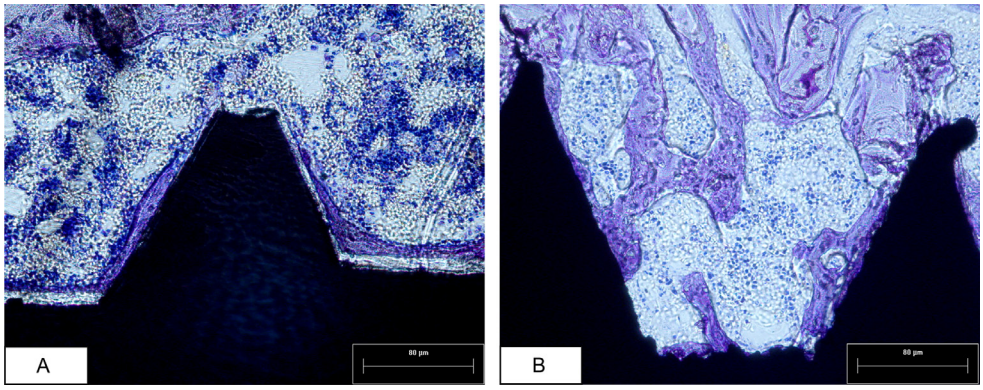

Fig. 5. Optical micrographs of implant surface samples after the 30-day bone-healing period. (A) shows newly deposited bone tissue near the surface of the machined implant with narrow space in bone/implant interface. (B) shows a laser treated implant surface with the distribution and direct contact of new trabecular bone on the implant surface. Toluidine blue staining.

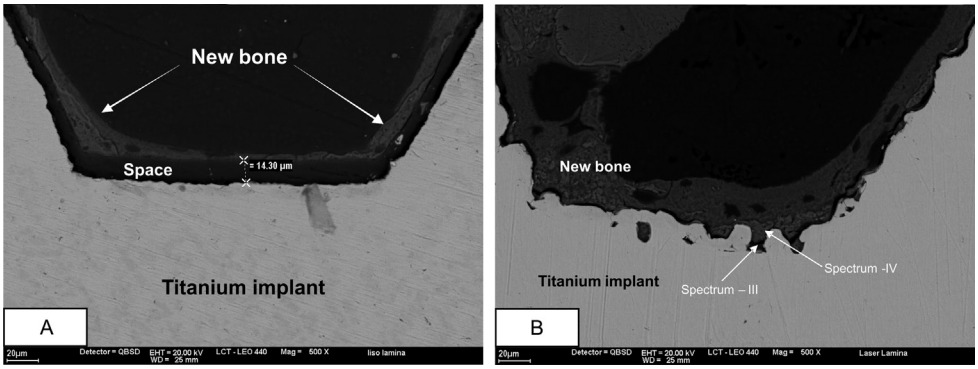

Fig. 6. (A) SEM image of a lamina of a machined implant sample after 30 days of bone healing. The newly deposited bone on the surface of the implant showed no contact with the implant. (B) SEM image of a laser-treated lamina after 30 days of bone healing. Space between two spirals revealed indentations caused by laser treatment. Spectra III and IV of the interface region between the surface of titanium and the newly deposited bone were obtained to identify the chemical components. Spectrum III was obtained from the recess region of a pore, and spectrum IV was obtained from the newly deposited bone tissue.

Average = 22.49; Laser Group – New Bone Average = 51.52). The laser-treated implants showed a higher level of significance when compared to simply machined surface implants ($p < 0.05$). However, comparative analysis between the groups at 30 and 60 days, showed no change in level of significance.

4. Discussion

A variety of titanium implant surface morphologies were examined to optimize cell-tissue interactions and, thus, to obtain early peri-implant bone deposition [19]. In recent studies [20,21] rough surfaces increased the contact area of implant/host bone, favoring improved peri-implant bone formation, compared to machined surfaces.

The macro and micro topography of the implant surface as well as the surface oxide layer on titanium have shown to be the main factors to positively influence osseointegration [4].

Major cellular activities during the repair process, *in vivo*, have been reported in studies where titanium implants, modified by different surface modification techniques, were evaluated [19,22–24].

In this study, increased trabecular bone repair was seen after 15 and 30 days in the implant samples that had their surfaces modified by laser beaming whereas after 60 days of bone repair there was a drop in the bone deposition process. SEM examinations indicated good interaction of the newly deposited tissue with the alterations on the surfaces treated with laser. Some studies, carried out with SEM, have shown that laser ablation of titanium surfaces resulted in a complex morphology, thus increasing the implant/bone contact interface [5,17,25]. Regarding the drop in bone matrix deposition

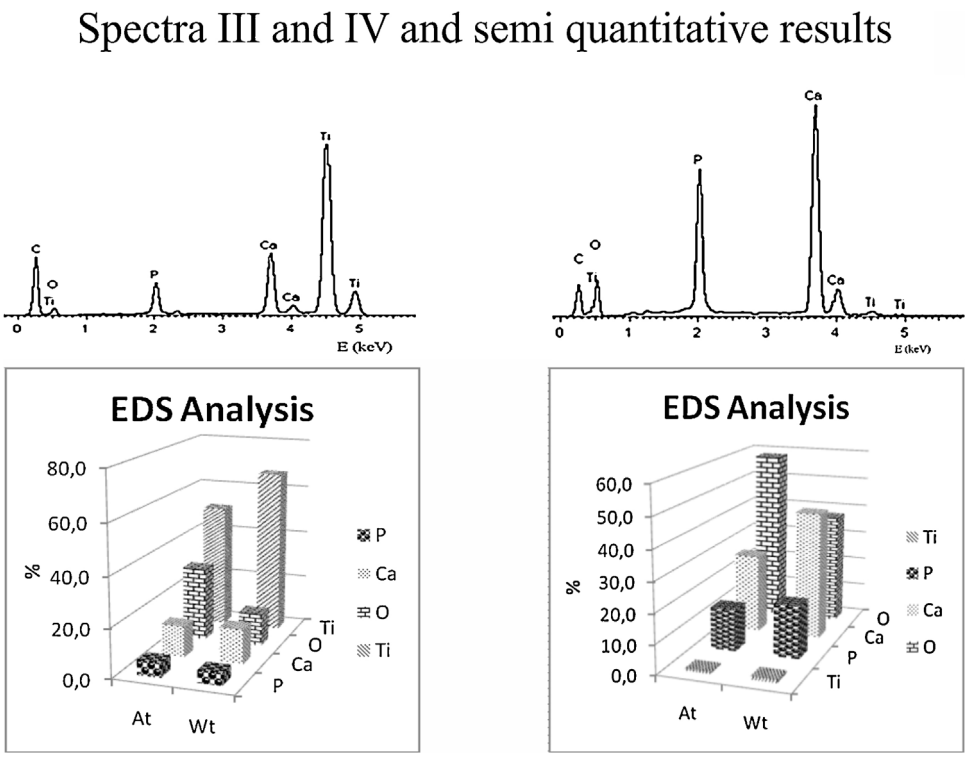

Fig. 7. Spectra III and IV of the new bone matrix deposition areas presented in Fig. 6B and semi-quantitative found through EDS analysis. At: Atomic Percent; Wt: Weight Percent; O: oxygen; Ti: Titanium; Ca: Calcium; P: Phosphorus.

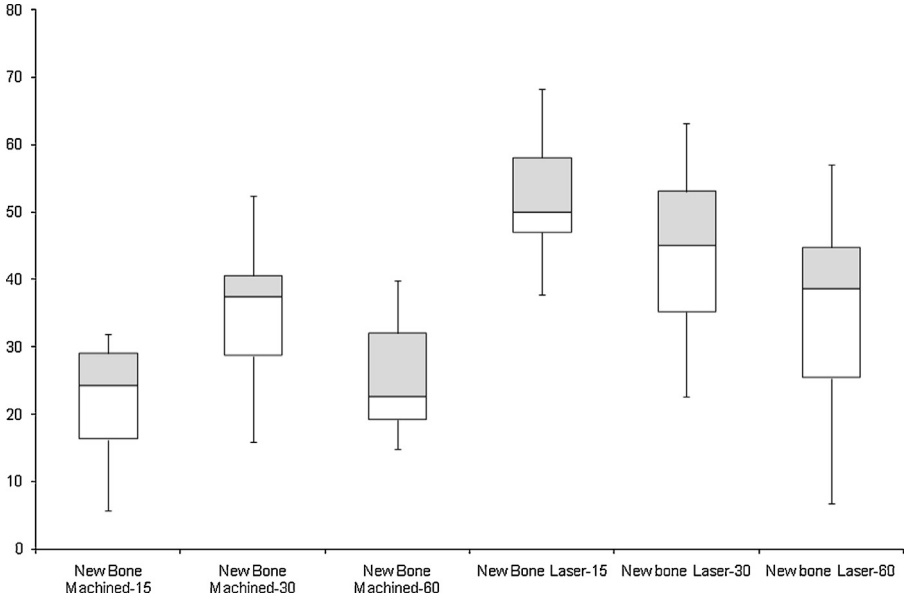

Fig. 8. Box-plot graphic created to demonstrate the distribution of the dataset obtained from histomorphometric analyses, considering variables, tolerance and mean values (Median). The observation of the data obtained for machined implant values shows little linearity among variables during the 15, 30 and 60-day healing periods and more representative results for the 30-day group. For the laser-treated group, a more symmetrical balance can be noticed among the values, confirming better values for the 15-day healing period.

observed in the 60-day healing periods, recent studies have shown suppressor of cytokine signaling 3 (SOCS3) to be a significant player in bone-associated inflammatory responses. Although the underlying mechanisms and signaling pathways regulating SOCS3 expression in osteoblasts and osteoclasts are still not quite well understood, it is known that they are involved with bone remodeling [26].

According to György et al. [12], the surface structure evolution is determined at the early stages of laser irradiation by hydrodynamic phenomena, and later by laser-induced thermochemical oxidation processes. Laser pulses when incident on surfaces promote release of heat, subsequent melting, decrease in surface reflectivity, rapid re-solidification forming a compact surface film and the formation of a porous oxide layer. Energy dissipation as well as rapid increase in temperature cause titanium to oxidize and the volume to increase. The volume increase can be attributed, in part, to the density difference between the Ti element and its oxides [27].

The architecture of an implant, and the size of pores on its surface, affect bone growth [28–30]. The ideal pore diameter for bone growth has been reported to be of 100–600 μm [29]. According to Hall et al. [28], pore width between 110 and 200 μm and depth of 70 μm stimulated good bone healing in an animal, while Guo et al. [30] reported pore diameter of 100 μm and pore depth between 80 and 100 μm to favor the growth of bone tissue. Results of this investigation have shown that laser treated implants had significant bone deposition after 15 and 30 days of bone repair even though their surfaces had only small diameter craters of reduced depth. This shows that it is not necessary to have large pores for good accommodation of new bone matrix. The laser treated surface showed direct contact with the mineralized and osteoid bone matrix, suggesting mechanical retention on the roughened surface. *In vitro* studies have suggested that surface morphology and the oxide layer promote deposition of bone apatite [3]. This *in vitro* formation on Ti surfaces in simulated body fluid was consistent with *in vivo* behavior of bone-implant union [22].

Some authors suggest that surface features at the micro and nano scale, enhanced by laser treatment, induce immediate and rapid bone formation at the interface. This results in bone union at a nano level, similar to that demonstrated recently in laser treated implants (Ti_6Al_4V) which had similar characteristics to those used in this experiment [5]. In other *in vivo* studies, the authors [17] concluded that surface features caused by laser surface treatment could promote improved approximation of bone cells, resulting in stronger bone-implant interfaces. The histomorphometric analysis in this current study demonstrated greater bone deposition in the early stages of repair process (15 days) for implants with laser-modified surfaces. This result may indicate that the morphological properties of such surfaces favor the approaching of cells.

Analysis of the laser treated surfaces through EDS showed that laser ablation resulted in an increase in oxygen content. This increase in oxygen ion content improved the thickness of the surface oxide layer and this may be one of the reasons for improved initial response in bone repair processes.

The occurrence of a local trauma in bone causes necrosis in parts of the existing tissue and vessel damage, impairing blood supply and consequent oxygen transport. Oxygen is the primary electron acceptor in many intracellular biochemical reactions and it is used by mitochondria to generate ATP through aerobic metabolism. Physiologically, the normal condition in terms of oxygen concentration is called “normoxia”. Concerning embryonic or adult cells, this concentration varies widely, but in the majority of cases it is set in the range of 2–9% O_2 (14.4–64.8 mm Hg) (air is 21% O_2) [31].

The results of the current study showed a greater volume of oxygen ions on the laser treated surface. This concentration of 13.9 at%, when compared to that on machined implants (4.4 at%), may be one reason for increased bone deposition in the early stages of tissue repair. The energy spectra obtained in the laser treated lamina of the femur showed 30.2 at% oxygen at the interface and 58.3 at% where new bone matrix deposition occurred. This highlights the fact that this element is essential for new bone matrix formation. However, at the interface, the higher concentration of this component can be attributed to bone proximity. As an analytical method, these changes are quite acceptable for conducting *in vivo* experiments and may serve as a baseline for comparisons with *in vitro* studies.

In *in vitro* studies using rat calvarial bone cells cultured under varying oxygen tensions, the authors concluded that cell proliferation was more significant with lower tension (less than or equal to 9% O_2) [32]. When progenitor stem cells of connective tissue

[33] and mesenchymal stem cells from bone marrow [34] were used, there was an increase in the Colony-Forming Efficiency (CFE) where such proliferation was more efficient when subject to strains of 5% O_2. Similar results were observed in human embryonic stem cells that showed improved proliferation when grown in 1–4% O_2, and was slightly lower with 1% O_2 [35]. In recent *in vitro* studies, authors concluded that an oxygen tension between 1 and 3% restores the osteogenic differentiation [36]. The rat mesenchymal stem cells grown under low O_2 also produce more osteocytes when implanted *in vivo* [31]. According to Burke et al. [37], mesenchymal cells, in particular, seem to be sensitive to a drop in oxygen tension. As O_2 can modulate cell fate in a concentration-dependent manner, it seems reasonable to assume that O_2 can perform similar functions to those of more traditionally recognized gradients of secreted growth factors [31].

The culture of populations of stem cells and undifferentiated cells must be concentrated in the 3–5% O_2 range [31]. Data from these articles indicate best results when the oxygen tension is higher. The concentration of oxygen on the laser treated implant surface, observed in this study, could explain proliferation of trabecular bone observed in the early stages of bone repair.

Studies of *in vitro* protocols and *in vivo* models (invertebrates and vertebrates) indicate that molecular O_2 is not just a fuel for maintenance of cellular metabolism and bioenergetics, but also an essential vehicle that regulates cell fate [31]. As mentioned above, the physiological "normoxia" is likely to be generally much lower than ambient air. Although most cells are maintained in culture conditions at 21% O_2, the oxygen tension must be low enough to influence and promote cell proliferation, and thereby improve the response of osteoblasts [31]. The necessary oxygen concentration in the surface layer of implants for increased responses requires further study.

5. Conclusions

Based on the results, we conclude that the roughness and oxide layer on the surfaces of laser-treated implants have provided improved response in bone repair when compared to implants with simply machined surfaces. Contact layers of new bone tissue on laser-treated implant surfaces after 15 and 30 days of bone repair were more evident when compared to machined implant surfaces. The higher oxygen concentration on the surface of laser treated implants possibly aided increased response of osteoblasts during the process of new bone matrix deposition.

Acknowledgements

We wish to thank the Nuclear Energy Institute at the University of São Paulo (IPEN/USP) for providing the material used in this research and for technical assistance. The research was partly funded by a fellowship from the Alexander von Humboldt Foundation for Dr. Sergio Allegrini Jr. (BRA/1115625).

References

[1] A. Neumann, K. Kevenhoerster, Biomaterials for craniofacial reconstruction, GMS Curr. Top. Otorhinolaryngol. Head Neck Surg. 8 (2009) 1–17.
[2] Y.H. Lin, P.W. Peng, K.L. Ou, The effect of titanium with electrochemical anodization on the response of the adherent osteoblast-like cell, Implant. Dent. 21 (2012) 344–349.
[3] T.J. Webster, J.U. Ejiofor, Increased osteoblast adhesion on nanophase metals: Ti, Ti6Al4V and CoCrMo, Biomaterials 25 (2004) 4731–4739.
[4] A.V. Xiropaidis, M. Qahash, W.H. Lim, R.H. Shanaman, M.D. Rohrer, U.M.E. Wikesjo, J. Hall, Bone-implant contact at calcium phosphate-coated and porous titanium oxide (TiUnite™) modified oral implants, Clin. Oral. Implants Res. 16 (2005) 532–539.
[5] A. Palmquist, F. Lindberg, L. Emanuelsson, R. Branemark, H. Engqvist, P. Thomsen, Biomechanical, histological, and ultrastructural analyses of laser micro- and nano structured titanium alloy implants: a study in rabbit, J. Biomed. Mater. Res. A 92 (2010) 1476–1486.
[6] S.K. Nishimoto, M. Nishimoto, S.W. Park, K.L. Lee, H.S. Kim, J.T. Koh, J.L. Ong, Y. Liu, Y. Yang, The effect of titanium surface roughening on protein absorption, cell attachment, and cell spreading, Int. J. Oral Maxillofac. Implants 23 (2008) 675–680.
[7] M. Simon, C. Lagneau, J. Moreno, M. Lissac, F. Dalard, B. Grosgogeat, Corrosion resistance and biocompatibility of a new porous surface for titanium implants, Eur. J. Oral Sci. 113 (2005) 537–545.
[8] L. Le Guéhennec, A. Soueidan, P. Layrolle, Y. Amouriq, Surface treatments of titanium dental implants for rapid osseointegration, Dent. Mater. 23 (2007) 844–854.
[9] R. Junker, A. Dimakis, M. Thoneick, J.A. Jansen, Effects of implant surface coatings and composition on bone integration: a systematic review, Clin. Oral. Implants Res. 20 (2009) 185–206.
[10] J.E. Davies, V.C. Mendes, J.C. Ko, E. Ajami, Topographic scale-range synergy at the functional bone/implant interface, Biomaterials 35 (2014) 25–35.
[11] M. Bereznai, I. Pelsoczi, Z. Toth, K. Turzo, M. Radnai, Z. Bor, A. Fazekas, Surface modifications induced by ns and sub-ps excimer laser pulses on titanium implant material, Biomaterials 24 (2003) 4197–4203.
[12] E. György, A. Pérez Del Pino, P. Serra, J.L. Morenza, Structure formation on titanium during oxidation induced by cumulative pulsed Nd:YAG laser irradiation, Appl. Phys. 78 (2004) 765–770.
[13] G. Olivi, M.D. Genovese, C. Caprioglio, Evidence-based dentistry on laser paediatric dentistry: review and outlook, Eur. J. Paediatr. Dent. 10 (2009) 29–40.
[14] C.M. Cobb, Lasers in periodontics: a review of the literature, J. Periodontol. 77 (2006) 545–564.
[15] C.M. Block, J.A. Mayo, G.H. Evans, Effects of the Nd:YAG dental laser on plasma-sprayed and hydroxyapatite coated titanium dental implants: surface alteration and attempted sterilization, Int. J. Oral Maxillofac. Implants. 7 (1992) 441–449.
[16] L. Lavisse, D. Grevey, C. Langlade, B. Vannes, The early stage of the laser-induced oxidation of titanium substrates, Appl. Surf. Sci. 186 (2002) 150–155.
[17] R.S. Faeda, H.S. Tavares, R. Sartori, A.C. Guastaldi, E. Marcantonio Jr., Evaluation of titanium implants with surface modification by laser beam, Biomechanical study in rabbit tibias, Braz. Oral Res. 23 (2009) 137–143.
[18] K. Donath, G. Breuner, Method for the study of undecalcified bones and teeth with attached soft tissues. The Säge schliff (sawing and grinding) technique, J. Oral Pathol. 11 (1982) 318–326.
[19] S. Lossdorfer, Z. Schwartz, L. Wang, C.H. Lohmann, J.D. Turner, M. Wieland, D.L. Cochran, B.D. Bovan, Microrough implant surface topographies increase osteogenesis by reducing osteoclast formation and activity, J. Biomed. Mater. Res. A 70 (2004) 361–369.
[20] A. Wennerberg, T. Albrektsson, Effects of titanium surface topography on bone integration: a systematic review, Clin. Oral. Implants Res. 20 (2009) 172–184.
[21] M.D. Paz, J.I. Álava, L. Goikoetxea, S. Chiussi, L. Días-Güemes, J. Usón, F. Sánchez, B. Leon, Biological response of laser macrostructured and oxidized titanium alloy: an in vitro and in vivo study, J. Appl. Biomater. Biomech. 9 (2011) 214–222.
[22] J.W. Park, I.S. Jang, J.Y. Suh, Bone response to endosseous titanium implants surface-modified by blasting and chemical treatment: a histomorphometric study in the rabbit femur, J. Biomed. Mater. Res. B Appl. Biomater. 84 (2008) 400–407.
[23] O. Omar, S. Svensson, N. Zoric, M. Lenneras, F. Suska, S. Wigren, J. Hall, U. Nannmark, P. Thomsen, *In vivo* gene expression in response to anodically oxidized versus machined titanium implants, J. Biomed. Mater. Res. A 92 (2010) 1552–1566.
[24] O. Omar, M. Lenneras, S. Svensson, F. Suska, L. Emanuelsson, J. Hall, U. Nannmark, P. Thomsen, Integrin and chemokine receptor gene expression in implant-adherent cells during early osseointegration, J. Mater. Sci. Mater. Med. 21 (2010) 969–980.
[25] J.A. Shibli, C. Mangano, S. D'avila, A. Piatelli, G.E. Pecora, F. Mangano, T. Onuma, L.A. Cardoso, D.S. Ferrari, K.C. Aguiar, G. Iezzi, Influence of direct laser fabrication implant topography on type IV bone: a histomorphometric study in humans, J. Biomed. Mater. Res. A 93 (2010) 607–614.
[26] A. Gao, T.E. Van Dyke, Role of suppressors of cytokine signaling 3 in bone inflammatory responses, Front Immunol. 10 (4) (2014) 506.
[27] A. Poulon-Quintin, L. Watanabe, E. Watanabe, C. Bertrand, Microstructure and mechanical properties of surface treated cast titanium with Nd:YAG laser, Dent. Mater. 28 (2012) 945–951.
[28] J. Hall, P. Miranda-Burgos, L. Sennerby, Stimulation of directed bone growth at oxidized titanium implants by macroscopic grooves: an *in vivo* study, Clin. Implant Dent. Relat. Res. 7 (2005) 76–82.
[29] B. Otsuki, M. Takemoto, S. Fujibayashi, M. Neo, T. Kokubo, T. Nakamura, Pore throat size and connectivity determine bone and tissue ingrowth into porous implants: three dimensional micro-CT based structural analyses of porous bioactive titanium implants, Biomaterials 27 (2006) 5892–5900.
[30] Z. Guo, L. Zhou, M. Rong, A. Zhu, H. Geng, Bone response to a pure titanium implant surface modified by laser etching and microarc oxidation, Int. J. Oral Maxillofac. Implants 25 (2010) 130–136.
[31] M.C. Simon, B. Keith, The role of oxygen availability in embryonic development and stem cell function, Nat. Rev. Mol. Cell Biol. 9 (2008) 285–296.

[32] C.T. Brighton, J.L. Schaffer, D.B. Shapiro, J.J. Tang, C.C. Clark, Proliferation and macromolecular synthesis by rat calvarial bone cells grown in various oxygen tensions, J. Orthop. Res. 9 (1991) 847–854.
[33] S.M. Villarruel, C.A. Boehm, M. Pennington, J.A. Bryan, K.A. Powell, G.F. Muschler, The effect of oxygen tension on the *in vitro* assay of human osteoblastic connective tissue progenitor cells, J. Orthop. Res. 26 (2008) 1390–1397.
[34] D.P. Lennon, J.M. Edmison, A.I. Caplan, Cultivation of rat marrow-derived mesenchymal stem cells in reduced oxygen tension: effects on *in vitro* and *in vivo* osteochondrogenesis, J. Cell Physiol. 187 (2001) 345–355.
[35] T. Ezashi, P. Das, R.M. Roberts, Low O_2 tensions and the prevention of differentiation of hES cells, Proc. Natl. Acad. Sci. U. S. A. 102 (2005) 4783–4788.
[36] C. Holzwarth, M. Vaegler, F. Gieseke, S.M. Pfister, R. Handgretinger, G. Kerst, I. Müller, Low physiologic oxygen tensions reduce proliferation and differentiation of human multipotent mesenchymal stromal cells, BMC Cell. Biol. 28 (2010) 1–11.
[37] D. Burke, M. Dishowitz, M. Sweetwyne, E. Miedel, K.D. Hankenson, D.J. Kelly, The role of oxygen as a regulator of stem cell fate during fracture repair in TSP2-null mice, J. Orthop. Res. 31 (2013) 1585–1596.